Journal of the European Ceramic Society **15** (1995) 503–511

0955-2219(95)00040-2
0955-2219/95/$9.50

Thermodynamic Assessment of the ZrO_2–$LaO_{1.5}$ System

Yong Du,* Masatomo Yashima, Toshiaki Koura, Masato Kakihana & Masahiro Yoshimura

Research Laboratory of Engineering Materials, Tokyo Institute of Technology, 4259 Nagatsuta, Midori-ku, Yokohama 226, Japan

(Received 2 June 1994; revised version received 7 February 1995; accepted 14 February 1995)

Abstract

Two optimal sets of thermodynamic functions for the ZrO_2–$LaO_{1.5}$ system are obtained by coupling the CALPHAD (CALculation of PHAse Diagrams) technique, the regularity between thermodynamic properties and crystal structure parameters within the family of rare earth oxides, and the Van't Hoff equation. The phases are modelled with the substitutional solution model (liquid, cubic, tetragonal, monoclinic, and hexagonal solid solutions), as the stoichiometric compounds ($Zr_{19}La_{42}O_{101}$, $Zr_2La_2O_7$), and with the sublattice model ($Zr_2La_2O_7$). Two optimizations are performed. In the first optimization, the $Zr_2La_2O_7$ phase is treated as a stoichiometric compound, while in the second one it is described by the Wagner–Schottky model. The eutectoid reaction, high-temperature hexagonal $LaO_{1.5}$ solid solution $\rightleftharpoons$ low-temperature hexagonal $LaO_{1.5}$ solid solution + $Zr_2La_2O_7$, is predicted from the calculation. The calculated phase diagrams and thermodynamic quantities agree well with the experimental data.

1 Introduction

It is well known that accurate thermodynamic information forms the basis of the CALPHAD method.[1–4] The current use of this method consists of evaluating a small number of thermodynamic parameters required to describe binary systems and synthesizing the description of a ternary system from the properties of its corresponding binary ones. The synthetic description for the ternary system can be used to evaluate existing experimental data and design experiments most efficiently. The same is true of going from ternary systems to a quaternary one and so on.

Recently the thermodynamic modelling of zirconia-bearing systems has received considerable attention[5–10] because of the difficulties[11,12] in constructing zirconia-based phase diagrams and thermodynamic properties by means of experimental methods, and the modelling has been justified by its ability to reproduce experimental data in binary systems and to predict experimental results in ternary systems with high certainty. It is interesting to notice that the calculated ZrO_2–$YO_{1.5}$–MgO phase diagrams[9] agree reasonably with most of the experimental data later published,[13,14] and the predicted ZrO_2–CaO–MgO and ZrO_2–$YO_{1.5}$–CaO phase diagrams[15,16] are in good agreement with the experimental data available. This means that the experimental work to measure zirconia ternary phase diagrams can be reduced significantly by using the CALPHAD method. In the case of experimentally well established zirconia binary systems, such as the ZrO_2–$YO_{1.5}$ and ZrO_2–CaO systems, consistent sets of thermodynamic parameters[17,18] can be obtained by only using the CALPHAD method. For most of the technologically important zirconia binary systems, however, experimental information is uncertain, scarce or lacking. Therefore, it is of great interest to optimize and/or estimate phase diagrams and thermodynamic properties in the less well established zirconia binary systems by the combined use of the CALPHAD technique and semiempirical estimation techniques. Similar work can be found for alloy systems, such as the work due to Guillermet and Frisk[19] and Klingbeil and Schmid-Fetzer.[20]

The present work is devoted to providing an optimal set of thermodynamic functions for the ZrO_2–$LaO_{1.5}$ system by coupling the CALPHAD method and semiempirical estimation techniques. This work is part of a research project aimed at developing a thermodynamic database for the ZrO_2–$REO_{1.5}$ (RE = Rare Earth)–CeO_2 systems, which is currently being carried out in our laboratory. The database is of great importance in the production and application of zirconia-based ceramic materials.

*Permanent address: Department of Materials Science and Engineering, Central South University of Technology, Changsha, Hunan, 410083, People's Republic of China.

2 Evaluation of Experimental Data

To conserve space, the cubic, tetragonal, and monoclinic structures of ZrO_2 and the low-temperature hexagonal, high-temperature hexagonal and cubic forms[21] of $LaO_{1.5}$ are denoted c-ZrO_2, t-ZrO_2, m-ZrO_2, A-$LaO_{1.5}$, H-$LaO_{1.5}$ and X-$LaO_{1.5}$, respectively. The solid solution phases based on c-ZrO_2, t-ZrO_2, m-ZrO_2, A-$LaO_{1.5}$, H-$LaO_{1.5}$ and X-$LaO_{1.5}$ are designated as C_{SS}, T_{SS}, M_{SS}, A_{SS}, H_{SS} and X_{SS}, respectively. All temperatures quoted in the present work have been converted into the international temperature scale of 1990.[22]

The liquidus for the ZrO_2–$LaO_{1.5}$ system has been measured by three groups of researchers.[23–25] The most detailed and accurate one is by Rouanet.[25] Except for one liquidus temperature at 38 mol% $LaO_{1.5}$ reported by Wartenberg and Eckhardt,[23] all of the liquidus data points published by them and Rouanet[25] are incorporated in the optimization. The qualitative liquidus data points given by Lin and Yu[24] cannot be used in the optimization.

Since Lefevre *et al.*[26] observed that the pyrochlore-type compound P ($Zr_2La_2O_7$) shows a homogeneity range, a few authors[27–30] have measured its range in a wide temperature range. However, the reported data show large scatter. All of the experimental values[26–30] were nevertheless retained in the optimization, since none of them alone can describe the homogeneity range satisfactorily. In addition to P, Rouanet[25,31] introduced another compound, C_2 (cubic-type Tl_2O_3). Qualitatively narrow range for C_2 has been reported, but definitive ranges are not given. Consequently, this compound is treated as a stoichiometric one, and its stoichiometric composition is palced at 68·8 mol % $LaO_{1.5}$, the average value of the two data points reported by Rouanet.[25,31]

Six groups of authors[24,25,30–33] contributed to the measurement of the solid state phase equilibria. Using X-ray diffraction (XRD) techniques, Brown and Duwez[32] determined the phase relations at 1623 and 2023 K, and Zheng and West[30] reported the phase relation at 1773 K. Based on XRD results, Lin and Yu[24] constructed the equilibrium diagram in the wide range of temperature and composition. All of the experimental values published by the above authors[24,30,32] are qualitative and cannot be utilized in the optimization. However, these data have been used as the checkpoints in the present assessment. By means of thermal analysis and XRD methods, Rouanet[25,31] measured the solidus curve, phase transition temperatures, and invariant equilibria. In the present optimization, all of the solid state phase equilibrium data reported by Rouanet[31] are used. Since the solidus curve is an estimated one and the reducing condition might affect temperature measurements associated with phase transitions, as pointed out by Wilder,[34] these data are attached a low weight in the optimization. Recently, Bastide *et al.*[33] measured the phase relation in the ZrO_2-rich part below about 1623 K in detail. The invariant data[33] for the reaction $T_{SS} \rightleftharpoons C_{SS} + P$ are employed in the optimization.

Using a bomb calorimeter, Korneev *et al.*[35] determined the enthalpy of formation of P at 298 K relative to the elements. This datum is included in the optimization.

3 Thermodynamic Models

3.1 Pure oxides ZrO_2 and $LaO_{1.5}$

The Gibbs free energy function ${}^0G(T) = G(T) - H^{SER}$ (lattice stability) of a pure oxide is expressed by the following equation:

$$ {}^0G(T) = A + BT + CT\ln T + DT^2 + ET^{-1} + FT^7 + GT^{-9} \quad (1) $$

in which H^{SER} is the weighted molar enthalpy of the stable element reference (SER), the pure element in its stable state at 298 K, and T the absolute temperature. For ZrO_2 and $LaO_{1.5}$, H^{SER} are $H^{SER}_{Zr} + 2H^{SER}_{O}$ and $H^{SER}_{La} + 1{\cdot}5H^{SER}_{O}$, respectively. The last two terms in Eqn (1) are used only outside the range of stability,[36] the term FT^7 for a liquid below melting point and GT^{-9} for solid phases above melting point.

As mentioned in the preceding section, $LaO_{1.5}$ has three modifications, A-$LaO_{1.5}$, H-$LaO_{1.5}$, and X-$LaO_{1.5}$. Experimental thermodynamic data are available only for A-$LaO_{1.5}$. In the present work, the lattice stability of A-$LaO_{1.5}$ is evaluated by the weighted least squares method[37] applied to the heat capacity[38–40] and enthalpy increment data.[41–43] The entropy and enthalpy of formation of $LaO_{1.5}$ at 298 K are taken from the recent compilation.[44] Based on the experimental results reported in Refs 21 and 45, the transition temperatures of A-$LaO_{1.5}$ $\rightleftharpoons$ H-$LaO_{1.5}$ and H-$LaO_{1.5}$ $\rightleftharpoons$ X-$LaO_{1.5}$ transitions and the melting temperature are placed at 2314 K, 2384 K, and 2584 K, respectively. The heat capacities of H-$LaO_{1.5}$ and liquid $LaO_{1.5}$ evaluated by Dinsdale[46] are adopted in the present work, and that of X-$LaO_{1.5}$ is assumed to be the average value of them. The H-$LaO_{1.5}$ $\rightleftharpoons$ X-$LaO_{1.5}$ transition enthalpy is estimated to be 29992 J/(mol of cation) by applying the Van't Hoff equation to the annotated ZrO_2–$LaO_{1.5}$ phase diagram.[31] Lacking further information, the A-$LaO_{1.5}$ $\rightleftharpoons$ H-$LaO_{1.5}$ transition enthalpy is assumed to be the same as that of the H-$YO_{1.5}$ $\rightleftharpoons$ C-$YO_{1.5}$ transition.[16,47] Ferro *et al.*[48] have demonstrated that within the family of the rare earth elements plus Y and Sc

constitutional properties (phase diagrams, thermodynamic properties and crystal structures) change according to a simple and systematic pattern. Regular trends of properties of trivalent rare earth oxides, such as transition temperatures[31] and enthalpy of formation of rare earth zirconates,[35] have been reported. In the present work, the enthalpy of melting of $LaO_{1.5}$ is extrapolated by plotting the experimental enthalpies of melting for $YO_{1.5}$[16,47] and $PrO_{1.5}$[44] vs the cation radii.[49] Table 1 lists the lattice stabilities employed in the present assessment.

3.2 Solution phases

Yin and Argent[8] have mentioned that the defect structures in zirconia-based systems are complicated, and for some systems, such as the ZrO_2–CaO system, the defect structure changes from anion vacancies to cation interstitials as temperature increases. Several groups of authors[6,8–10] have shown that the simple substitutional solution model used for metal systems can describe the ZrO_2-based systems satisfactorily. When this model is used to describe solution phases in ZrO_2-bearing systems, it means that clusters, such as associates and neutral species, are not introduced in thermodynamic modelling, and cations and anions were in their simplest forms, such as Zr^{+4}, La^{+3}, O^{-2}. In accordance with the substitutional solution model, the Gibbs free energy of the liquid is expressed by an equation of the form:

$$G^{L}_{m}-H^{SER} = x^{0}G^{L}_{LaO_{1.5}} + (1-x)^{0}G^{L}_{ZrO_2} + RT [x \ln x + (1-x) \ln (1-x)] + x(1-x)[a_0 + b_0T + (a_1 + b_1T)(1-2x) + \ldots] \quad (2)$$

where x is the mole fraction of $LaO_{1.5}$, and R the gas constant. The remaining solution phases are defined in a fashion similar to Eqn (2).

In view of the narrow homogeneity range for C_2, this compound is treated as a stoichiometric one, and its Gibbs free energy is expressed relative to the constituent oxides by the following equation:

$$G^{C_2}_{0.312(ZrO_2)\,0.688(LaO_{1.5})} - H^{SER} = 0.688\,{}^{0}G^{C_2}_{LaO_{1.5}} + 0.312\,{}^{0}G^{C_2}_{ZrO_2} + A + BT \quad (3)$$

In the first optimization, P is also modelled as a stoichiometric compound. For P, the enthalpy of formation at 298 K has been measured.[35] This quantity is directly expressed by A of Eqn (3), if the reference states of ZrO_2 and $LaO_{1.5}$ correspond to the states to which the measured enthalpy of formation is referred. Therefore, it is preferable to choose m-ZrO_2 and A-$LaO_{1.5}$ as the reference states in the Gibbs free energy expression of P.

In the second optimization, the homogeneity range for P is considered. If it is assumed that the cations and anions were in their simplest forms, the two sublattices $(ZO,LO)_1(LO,ZO)_1$ described by the Wagner–Schottky formalism[50] could be used to model this compound. ZO and LO are the abbreviations of ZrO_2 and $LaO_{1.5}$, respectively. According to the Wagner–Schottky formalism, the Gibbs free energy of P is given by the following expression:

$$G - H^{SER} = 0.5\,{}^{0}G^{pyro}_{ZrO_2} + 0.5\,{}^{0}G^{pyro}_{LaO_{1.5}} + RT[0.5\{Y'_{Lo} \ln Y'_{Lo} + (1-Y'_{Lo}) \ln (1-Y'_{Lo})\} + 0.5\{Y''_{Lo} \ln Y''_{Lo} + (1-Y''_{Lo}) \ln (1-Y''_{Lo})\}] + G^{*} + G_{12}n_{12} + G_{21}n_{21} \quad (4)$$

Table 1. Summary of lattice stability parameters[a]

$G^{L\text{-}LaO_{1.5}} - H^{SER}_{La} - 1.5H^{SER}_{O}$
$298 < T < 2584 = -822856.8 + 304.7303T - 59.8354T \ln T - 0.0036025T^2 + 342279.5T^{-1} - 1.7315 \times 10^{-21}T^7$
$2584 < T < 6000 = -894331.4 + 638.1947T - 100T \ln T$

$G^{X\text{-}LaO_{1.5}} - H^{SER}_{La} - 1.5H^{SER}_{O}$
$298 < T < 2584 = -915282 + 567.7316T - 90T \ln T$
$2584 < T < 6000 = -943993.1 + 657.3025T - 100T \ln T + 1.474628 \times 10^{33}T^{-9}$

$G^{H\text{-}LaO_{1.5}} - H^{SER}_{La} - 1.5H^{SER}_{O}$
$298 < T < 2584 = -921434 + 492.5469T - 80T \ln T$
$2584 < T < 6000 = -978856.5 + 671.6888T - 100\,T \ln T + 2.949257 \times 10^{33}T^{-9}$

$G^{A\text{-}LaO_{1.5}} - H^{SER}_{La} - 1.5H^{SER}_{O}$
$298 < T < 2584 = -917924.2 + 343.0925T - 59.8354T \ln T - 0.0036025T^2 + 342279.5T^{-1}$
$2584 < T < 6000 = -1003606 + 682.3301T - 100T \ln T + 3.192479 \times 10^{33}T^{-9}$

$G^{t\text{-}LaO_{1.5}} - H^{SER}_{La} - 1.5H^{SER}_{O}$
$298 < T < 6000 = G^{l\text{-}LaO_{1.5}} - H^{SER}_{La} - 1.5H^{SER}_{O} - 35617.5 + 26.4625T$

$G^{m\text{-}LaO_{1.5}} - H^{SER}_{La} - 1.5H^{SER}_{O}$
$298 < T < 6000 = G^{l\text{-}LaO_{1.5}} - H^{SER}_{La} - 1.5H^{SER}_{O} - 14697.5 + 29.915T$

$G^{H\text{-}ZrO_2} - H^{SER}_{Zr} - 2H^{SER}_{O}$
$298 < T < 6000 = G^{L\text{-}ZrO_2} - H^{SER}_{Zr} - 2H^{SER}_{O} - 71547 + 28.188T$

[a]In J/(mol of cation); temperature (T) in kelvin. L is liquid, X is cubic $LaO_{1.5}$, H is high-temperature hexagonal $LaO_{1.5}$, A is low-temperature hexagonal $LaO_{1.5}$, t is tetragonal ZrO_2 and m is monoclinic ZrO_2. The stable lattice stabilities of ZrO_2 are taken from the recent evaluation by Du *et al.*[18] Lacking further information, it is assumed that the Gibbs free energy difference between L–ZrO_2 and H (A)-ZrO_2 is the same as that[6] of HfO_2.

in which ${}^0G^{pyro}_{ZrO_2}$ and ${}^0G^{pyro}_{LaO_{1.5}}$ are the Gibbs energies of ZrO_2 and $LaO_{1.5}$ in the pyrochlore structure, respectively. Y'_{LO} and Y''_{LO} are the site fractions of the species LO on the first and second sublattices, respectively. G^* is the Gibbs energy of formation of the ideal compound ($Zr_2La_2O_7$), and G_{21} and G_{12} are the Gibbs energies of formation of the fictitious compounds, ZO_1:ZO_1 and LO_1:LO_1, respectively. The colon indicates the end of first sublattice and the start of the second one. n_{ij} is the number of moles of species j on sublattice i.

4 Parameter Evaluation

For convenience, the first and second optimizations in which P is treated as a stoichiometric compound and modelled with the Wagner–Schottky formalism, are referred to as optimizations A and B, respectively. For both optimizations, the other experimental values input are the same.

The evaluation of the parameters is conducted by the program developed by Lukas *et al.*[2] For the liquid it is possible to adjust independently the coefficients a_0 and b_0 of Eqn (2), because the liquidus line has been measured accurately over the whole composition range. In the present work, it was found that the calculated liquidus lines introducing and without introducing b_0 nearly coincide. So in the final optimization, only a_0 was used. The terminal solid solutions C_{SS} and X_{SS} both are cubic[21] and are treated as the same phase in the thermodynamic modelling. The coefficients a and b of Eqn (2) for C_{SS}(X_{SS}) cannot be adjusted independently due to the less well established temperature dependence. To make the excess enthalpy of $LaO_{1.5}$-rich solid solution (X_{SS}) independent from that of ZrO_2-rich solid solution (C_{SS}), a_0 and a_1 need to be introduced. Since the experimental data associated with T_{SS}, H_{SS} and X_{SS} are limited and scatter, each of them is described by one regular parameter. In view of the low solubility of $LaO_{1.5}$ in m-ZrO_2 (0·9 mol % $LaO_{1.5}$ at 1373 K), M_{SS} was approximated as m-ZrO_2. For C_2, it is impossible to adjust A and B of Eqn (3) independently because its Gibbs energies are known only in a narrow temperature range. Since only one coefficient can be adjusted, the value of B was fixed to be 2·75 J/(mol of cation·K). When this value is converted into that corresponding to one mole atom, it is about 1 J/(mol of atom K), which is usually adopted in the assessment of metal systems.[51] In the case of P, the coefficients A and B can be adjusted in optimization A, since the enthalpy of formation and phase diagram data are available. For optimization B, the introduction of two coefficients for G^* and one coefficient for each of G_{12} and G_{21} gives a good compromise to the scatter homogeneity range. The thermodynamic parameters obtained in the present work are shown in Table 2 (optimization A) and Table 3 (optimization B).

5 Results and Discussion

In Fig. 1, the calculated heat capacity of A-$LaO_{1.5}$ is compared with the experimental values.[38–40] Except for the two data points[40] at 800 and 850 K, all of the other experimental values can be reproduced by the calculation within the estimated experimental errors. Basili *et al.*[40] gave a large uncertainty (5%) for their heat capacity data. The large uncertainty corresponds to a low weight in the weighted least squares method.[37] The comparison of the calculated enthalpy increment and the experimental points[41–43] for A-$LaO_{1.5}$ is presented in Fig. 2, which shows a very good agreement.

The estimated enthalpy of melting of $LaO_{1.5}$ is shown in Fig. 3 along with the experimental ones for $YO_{1.5}$[16,47] and $PrO_{1.5}$.[44] In Fig. 3(a), the crystal radius[49] is used, while in Fig. 3(b) the effective ionic radius[49] is utilized. As can be seen from the figures, the estimated enthalpies of melting of $LaO_{1.5}$ are nearly the same in spite of the use of a

Table 2. Optimized thermodynamic parameters for the ZrO_2–$LaO_{1.5}$ system from optimization A (P is modelled as a stoichiometric compound)[a]

Substitutional solution model (Eqn (2))

Phase	i	a_i	b_i	Phase	i	a_i	b_i
Liquid	0	−108326·1	0	C_{SS}(X_{SS})	0	−64239·9	0
T_{SS}	0	−97316·9	0		1	−4658·5	0
A_{SS}	0	−17923·1	0	H_{SS}	0	−52500·6	0

Stoichiometric model (Eqn (3))

Phase	A	B	Phase	A	B
[b]C_2	−83478·8	2·75	P	−54173·8	6·26749

[a] In J/(mol of cation). C_{SS} and T_{SS} are cubic and tetragonal ZrO_2 solid solutions, respectively. X_{SS}, H_{SS} and A_{SS} are the solid solutions based on cubic, high- and low-temperature hexagonal $LaO_{1.5}$, respectively. C_2 and P are $Zr_{19}La_{42}O_{101}$ and $Zr_2La_2O_7$, respectively.
[b] Lacking further information, the Gibbs energy differences for both ZrO_2 and $LaO_{1.5}$ in the cubic-type Tl_2O_3 are simply given a fixed large value (50000 J/(mol of cation)) compared to c-ZrO_2 and X-$LaO_{1.5}$.

Table 3. Optimized thermodynamic parameters for the ZrO_2–$LaO_{1.5}$ system from optimization B (P is modelled with the sublattice model)[a]

Substitutional solution model (Eqn (2))

Phase	i	a_i	b_i	Phase	i	a_i	b_i
Liquid	0	-92098·4	0	$C_{SS}(X_{SS})$	0	-46929·2	0
T_{SS}	0	-77847·9	0		1	-3387·7	0
H_{SS}	0	-34929·3	0				

Stoichiometric model (Eqn (3))

Phase	A	B
C_2	-80286	2·75

Sublattice model (Eqn (4))

Phase	G^*	G_{12}	G_{21}
[b]P	-35126·9 + 1·34452T	-102327	-101998

[a] In J/(mol of cation); Temperature (T) in kelvin. For abbreviations of the phases, see Table 2.
[b] Due to the lack of experimental information, the Gibbs energy differences for both ZrO_2 and $LaO_{1.5}$ in the pyrochlore structure are simply given a fixed large value (100000 J/(mol of cation)) compared to m-ZrO_2 and A-$LaO_{1.5}$.

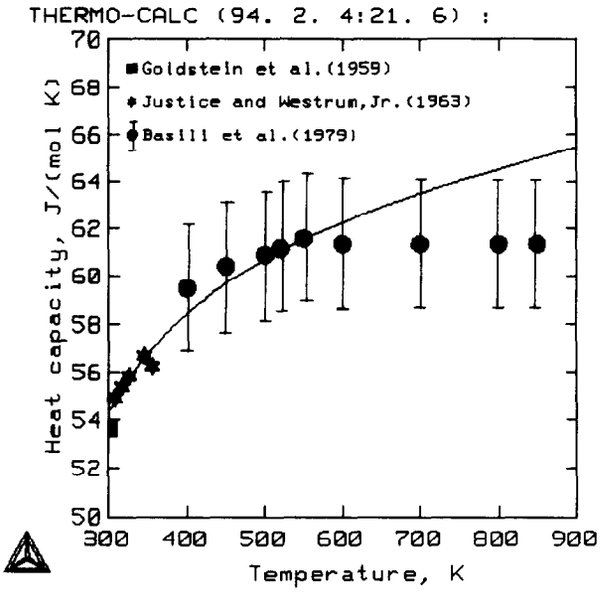

Fig. 1. Comparison of the calculated and measured[38-40] heat capacities of $LaO_{1.5}$.

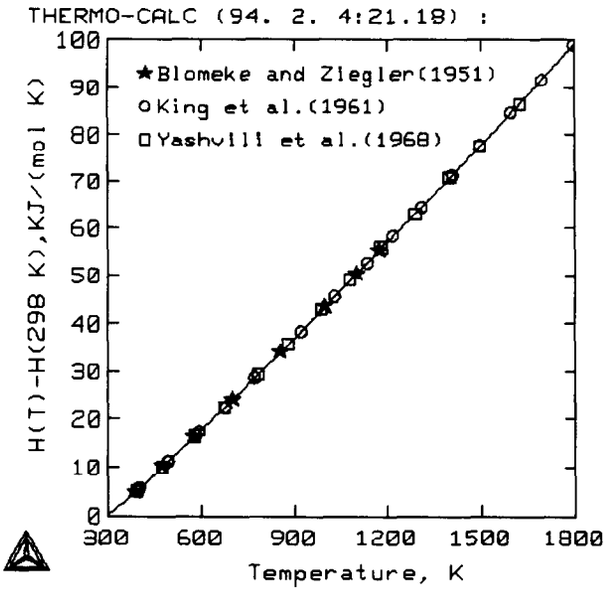

Fig. 2. Calculated enthalpy increment of $LaO_{1.5}$ with the experimental values.[41-43]

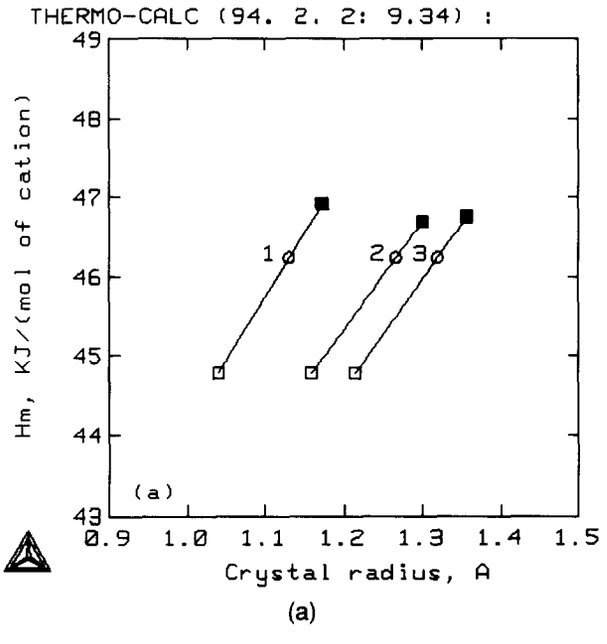

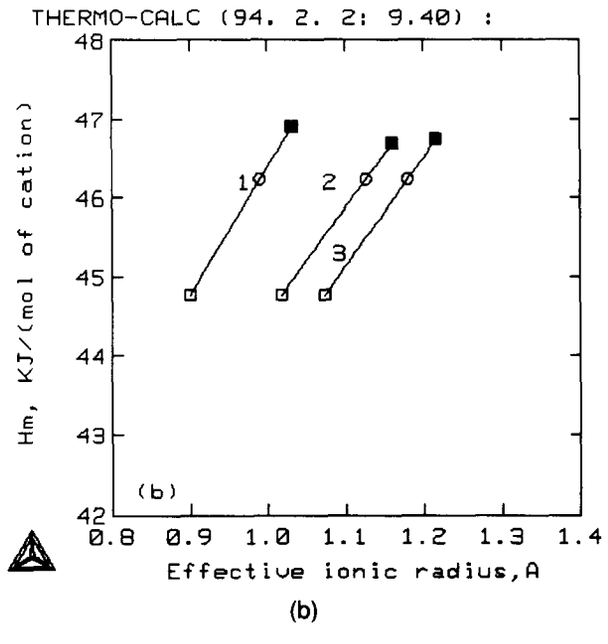

Fig. 3. Estimated enthalpy of melting of $LaO_{1.5}$ (■) along with the experimental enthalpies for $YO_{1.5}$ (□)[16,47] and $PrO_{1.5}$ (○).[44] Curves 1, 2, and 3 correspond to the coordination numbers 6, 8 and 11, respectively. (a) Enthalpy of melting is plotted vs crystal radius, and (b) enthalpy of melting is plotted vs effective ionic radius.

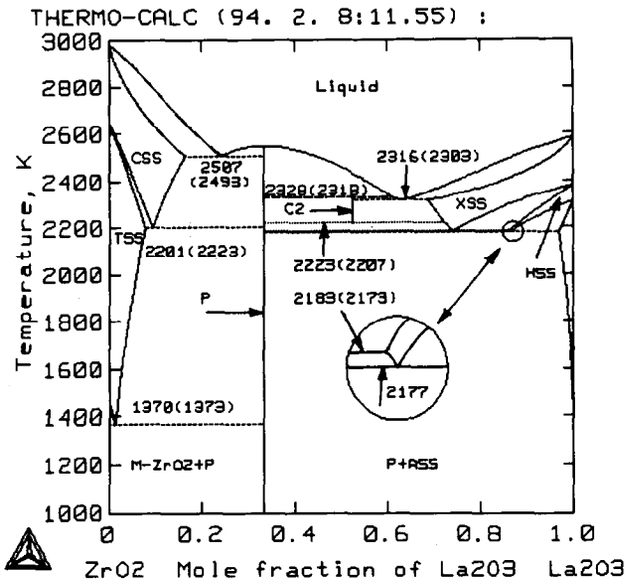

Fig. 4. Calculated ZrO_2–La_2O_3 phase diagram according to optimization A. The temperatures inside the parentheses are the experimental invariant temperatures,[31] and those outside the parentheses are the calculated ones.

different cation radius and a different coordination number. The average value (46790·7 J/(mol of cation)) of the six data points is taken to be the enthalpy of melting. The enthalpy of melting of $LaO_{1.5}$ calculated statistically from related phase diagrams, using the Van't Hoff equation, gives rise to the value of about 35000 J/(mol of cation), which is comparative with that assessed in the present work. Considering the large uncertainty (about 30%) associated with the Van't Hoff equation, the presently estimated value is preferable.

The presently calculated enthalpies of formation of P at 298 K from the elements are -1053187 J/(mol of cation) (optimization A) and -1036303 J/(mol of cation) (optimization B), which agree reasonably with the experimental one (-1020478 J/(mol of cation).[35]

The complete ZrO_2–La_2O_3 phase diagram based on optimization A is shown in Fig. 4. The eutectoid reaction, $H_{SS} \rightleftharpoons P + A_{SS}$, is a result of the calculation. No experimental information is available about this reaction. For the other invariant equilibria, the fit to the experimental data[31] is very good within the estimated errors.

In Fig. 5, the calculated ZrO_2–La_2O_3 phase diagram resulting from optimization A is compared with all of the experimental data available. Except for the homogeneity data for P, most of the other experimental data can be described by the calculation. In particular, the quantitative experimental values[23,25,31,33] are well reproduced. The calculated solidus line in ZrO_2-rich part is a little lower than the estimated one.[31] The present calculation demonstrated that the qualitative liquidus and solidus curves given by Lin and Yu[24] are probably low. Lin and Yu reported the melting temperature of $LaO_{1.5}$ to be 2533 K, which is lower by 51 K than the generally accepted one (2584 K).

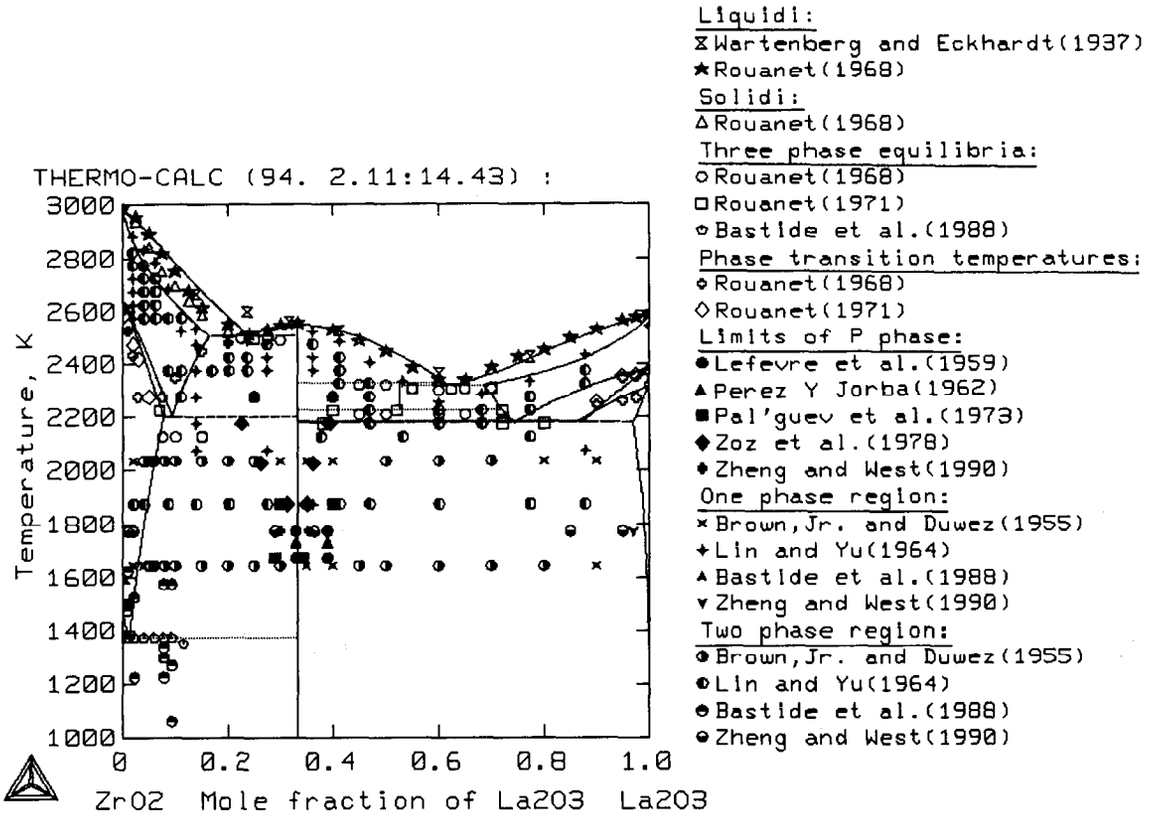

Fig. 5. Calculated ZrO_2–La_2O_3 phase diagram with the experimental phase diagram data. $Zr_2La_2O_7$ is treated as a stoichiometric compound (optimization A).

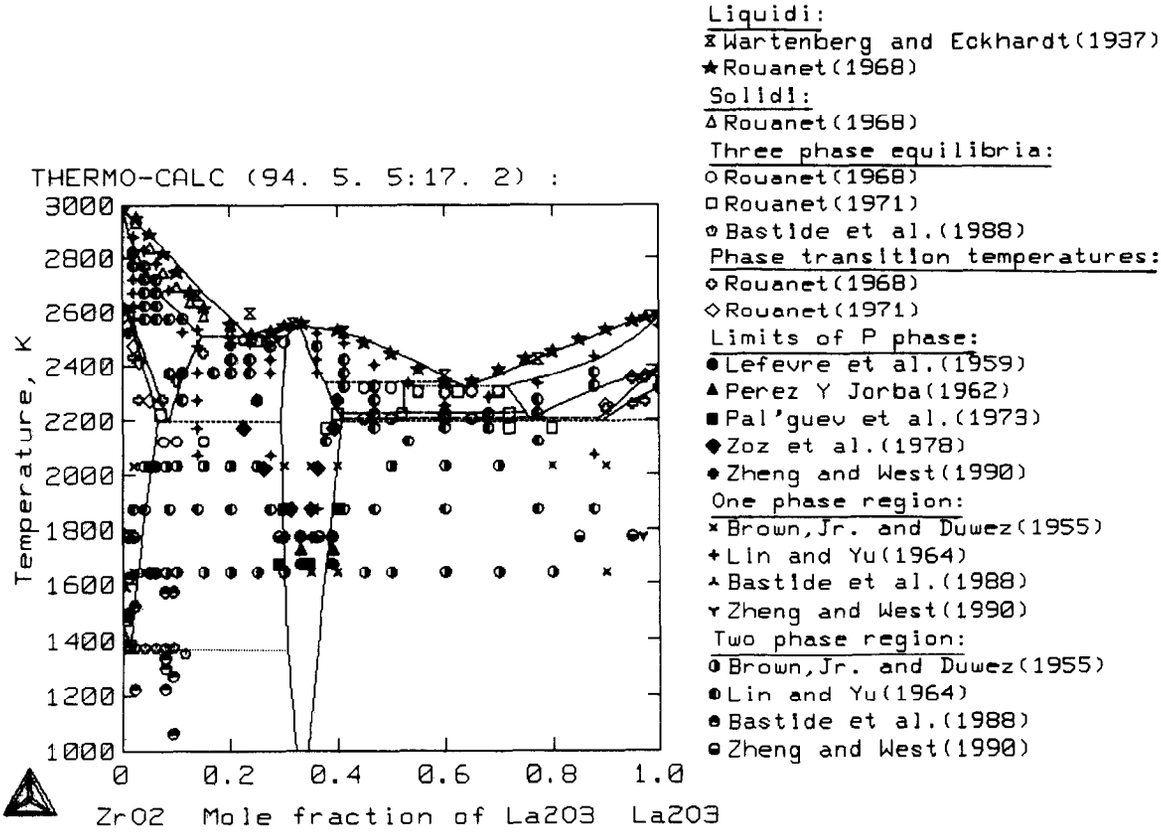

Fig. 6. Calculated ZrO_2–La_2O_3 phase diagram with the experimental phase diagram data. $Zr_2La_2O_7$ is modelled with the sublattice model (optimization B).

The computed ZrO_2–La_2O_3 phase diagram according to optimization B is presented in Fig. 6, which demonstrates an excellent fit to the quantitative experimental data[21,25,31,33] The calculated homogeneity range for P is a good compromise to the available data.[26–30] As mentioned in Section 2, the experimental data for the range of P show large scatter. The calculated limit toward La_2O_3 is located approximately at a curve between the curve reported by Lefevre *et al.*,[26] Perez Y Jorba[27] and Pal'guev *et al.*[28] and the one determined by Zoz *et al.*[29] and Zheng and West.[30] In the case of the limit toward ZrO_2, the computed limit agrees reasonably with the results from Pal'guev *et al.*,[28] Zheng and West,[30] and the datum at 1873 K published by Zoz *et al.*[29] The experimental result given by Lefevre *et al.*[26] and Perez Y Jorba[27] is higher by about 3 mol% La_2O_3 than the calculated one. In contrast, the experimental data at 2023 K and 2173 K given by Zoz *et al.*[29] are lower by about 5 mol% La_2O_3 than the computed one. Better knowledge on the homogeneity range of P is useful for further refinement of the ZrO_2–$LaO_{1.5}$ system. In the case of optimization B, it is found that the calculated solubility of ZrO_2 in $LaO_{1.5}$ is significantly lower than one quantitative datum published by Zheng and West.[30] An attempt to improve the agreement with this datum results in worse agreement with the phase transition temperatures and homogeneity range of P. In consequence, A_{SS} is approximated as A-$LaO_{1.5}$ in the final optimization. In the present work, an attempt to model P with the substitutional solution model was not successful: the calculated homogeneity range deviates significantly from the experimental data.[26–30] This implies the inapplicability of the substitutional solution model to describe P. The substitutional solution model corresponds to the random mixing of two species (ZrO_2, $LaO_{1.5}$) in one sublattice. This is not the case for $Zr_2La_2O_7$. The present work demonstrates that two sublattice model can be used to describe this compound.

The thermodynamic description of the ZrO_2–$LaO_{1.5}$ system obtained in the present work has been combined with the thermodynamic parameters for the ZrO_2–CeO_2[52] and CeO_2–$LaO_{1.5}$ systems to predict the ZrO_2–CeO_2–$LaO_{1.5}$ ternary phase diagrams, which are in reasonable agreement with the experimental data available.

6 Summary

All the phase diagram and thermodynamic data available for the ZrO_2–$LaO_{1.5}$ system have been considered in the present assessment. An attempt has been made to provide the consistent set of thermodynamic parameters describing the system

by coupling CALPHAD method and semiempirical estimation techniques. Two sets of thermodynamic functions have been obtained in the present work. The first one is for a simplified version of the ZrO_2–$LaO_{1.5}$ phase diagram in which $Zr_2La_2O_7$ is treated as a stoichiometric compound. The second one corresponds to the treatment in which $Zr_2La_2O_7$ is modelled with the sublattice model. Comprehensive comparisons with the experimental data available are made, and it is shown that the first parameter set can satisfactorily account for most of the experimental data except for the homogeneity data of $Zr_2La_2O_7$, and the second parameter set gives a good fit to all types of data for the ZrO_2–$LaO_{1.5}$ system except for one solubility datum of ZrO_2 in $LaO_{1.5}$.

Acknowledgements

The use of the program from Dr H. L. Lukas is gratefully acknowledged. One of the authors (Yong Du) is grateful to Professor M. Yoshimura for his nomination to the 29th International Course in Chemistry and Chemical Engineering and to Professors P. Y. Huang, Z. P. Jin and B. Y. Huang for their recommendations to the Course. Partial support from Iketani Science and Technology Foundation are also acknowledged.

References

1. Kaufman, L. & Bernstein, H., *Computer Calculation of Phase Diagrams.*, Academic Press, New York, 1970.
2. Lukas, H. L., Henig, E. -Th. & Zimmermann, B., Optimization of phase diagrams by a least squares method using simultaneously different types of data. *CALPHAD: Comput. Coupling Phase Diagrams Thermochem.*, **1** (1977) 225–36.
3. Pelton, A. D., Computer coupling of phase diagrams and thermodynamics. *Ber. Bunsenges. Phys. Chem.*, **87** (1983) 183–8.
4. Sundman, B., Jansson, B. & Andersson, J. -O., The Thermo Calc databank system. *CALPHAD: Comput. Coupling Phase Diagrams Thermochem.*, **9** (1985) 153–90.
5. Yoshimura, M., Tani, E. & Somiya, S., The confirmation of phase equilibria in the system ZrO_2–CeO_2 below 1400°C. *Solid State Ionics*, **3/4** (1981) 477–81.
6. Kaufman, L., Calculation of multicomponent ceramic phase diagrams. *Physica B+C: (Amsterdam)*, **150** (1988) 99–114.
7. Wu, P., Eriksson, G. & Pelton, A. D., Optimization of the thermodynamic properties and phase diagrams of the Na_2O–SiO_2 and K_2O-SiO_2 systems. *J. Am. Ceram. Soc.*, **76** (1993) 2059–64.
8. Yin, Y. & Argent, B. B., Phase diagrams and thermodynamics of the systems ZrO_2–CaO and ZrO_2–MgO. *J. Phase Equilibria*, **14** (1993) 439–50.
9. Du, Y., Jin, Z. P. & Huang, P. Y., Thermodynamic calculation of the ZrO_2–$YO_{1.5}$–MgO system. *J. Am. Ceram. Soc.*, **74** (1991) 2107–12.
10. Yokokawa, H., Sakai, N., Kawada, T. & Dokiya, M., Phase diagram calculations for ZrO_2 based ceramics: thermodynamic regularities in zirconate formation and solubilities of transition metal oxides. In *Science and Technology of Zirconia V*, ed. S. P. S. Badwal, M. J. Bannister & R. H. J. Hannink. Technomic Publishing Company, Inc., Lancaster, PA 17604, USA, 1993, pp. 59–68.
11. Stubican, V. S. & Hellmann, J. R., Phase equilibria in some zirconia systems. In *Science and Technology of Zirconia*, ed. A. H. Heuer & L. W. Hobbs. American Ceramic Society, Columbus, OH, USA, 1981, pp. 25–37.
12. Yoshimura, M., Phase stability of zirconia. *Am. Ceram. Soc. Bull.*, **67** (1988) 1950–5.
13. Lopato, L. M., Gerasimyuk, G. I., Shevchenko, A. V. & Karpenko, Yu. M., Interaction in the zirconia–yttria–magnesia system. *Izv. Akad. Nauk SSSR, Neorg. Mater.*, **27** (1991) 992–5.
14. Shevchenko, A. V., Lopato, L. M., Karpenko, Yu. M., Gerasimyuk, G. I. & Ruban, A. K., Liquidus surface and polythermal crossections of the zirconia–yttria–magnesia system. *Izv. Akad. Nauk SSSR, Neorg. Mater.*, **27** (1991) 996–1000.
15. Du, Y., Jin, Z. P. & Huang, P. Y., Calculation of the ZrO_2–CaO–MgO phase diagram. *CALPHAD: Comput. Coupling Phase Diagrams Thermochem.*, **16** (1992) 221–30.
16. Jin, Z. P. & Du, Y., Thermodynamic calculation of the ZrO_2–$YO_{1.5}$–CaO phase diagram. *CALPHAD: Comput. Coupling Phase Diagrams Thermochem.*, **16** (1992) 355–62.
17. Du, Y., Jin, Z. P. & Huang, P. Y., Thermodynamic assessment of the ZrO_2–$YO_{1.5}$ system. *J Am. Ceram. Soc.*, **74** (1991) 1569–77.
18. Du, Y., Jin, Z. P. & Huang, P. Y., Thermodynamic calculation of the zirconia–calcia system. *J. Am. Ceram. Soc.*, **75** (1992) 3040–8.
19. Guillermet, A. F. & Frisk, K., Thermodynamic properties of Ni nitrides and phase stability in the Ni–N system. *Int. J. Thermophys.*, **12** (1991) 417–31.
20. Klingbeil, J. & Schmid-Fetzer, R., Terquat: approximate prediction of ternary and quaternary phase diagrams comprising stoichiometric phases. *J. Phase Equilibria*, **13** (1992) 522–31.
21. Foex, M. & Traverse, J. P., Remarques sur les transformations cristallines présentées a haute température par les sesquioxydes de terres rares. *Rev. Int. Hautes Temp. Refract.*, **3** (1966) 429–53.
22. Thomas, H. P., The international temperature scale of 1990 (ITS-90). *Metrologia*, **27** (1990) 3–10.
23. Wartenberg, H. V. & Eckhardt, K., Schmelzdiagramme hochstfeuerfester oxyde. VIII. Systeme mit CeO_2. *Z. Anorg. Allgem. Chem.*, **232** (1937) 179–87.
24. Lin, T. H. & Yu, H. C., Phase equilibria of systems Ln_2O_3 (Rare Earth Oxides) –ZrO_2. I. phase equilibria of the binary system La_2O_3–ZrO_2. *J. Chin. Ceram. Soc.*, **3** (1964) 159–66 (in Chinese).
25. Rouanet, A., Étude de la refractairité et de la structure des phases de haute température présentées par le système zircone–oxyde de lanthane. *C. R. Acad. Sci., Paris, Ser. C*, **267** (1968) 395–7.
26. Lefevre, J., Perez Y Jorba, M. & Collongues, R., Sur les diagrammes d'équilibre zircone–oxydes de terres rares. *Bull. Soc. Chim. France*, **5** (1959) 1969–71.
27. Perez Y Jorba, M., Contribution a l'étude des systèmes zircone–oxydes de terres rares. *Ann. Chim.*, **7** (1962) 479–51.
28. Pal'guev, S. F., Fomina, L. N. & Strekalovskii, V. N., Thermal X-ray diffraction study of the reaction of zirconium dioxide and lanthanum oxide in the region of ccurrence of $La_2Zr_2O_7$. *Tr. Inst. Elektrokhim., Ural. Nauchn. Tsentr. Akad. Nauk SSSR*, **19** (1973) 120–7.
29. Zoz, E. I., Gavrish, A. M. & Gul'ko, N. V., Phase formation in the zirconium oxide (hafnium oxide)–lanthanum oxide systems. *Izv. Akad. Nauk SSSR, Neorg. Mater.*, **14** (1978) 109–11.
30. Zheng, C. & West, A. R., Phase equilibria and electrical properties in the system ZrO_2–La_2O_3–Nd_2O_5. *Br. Ceram. Trans. J.*, **89** (1990) 138–41.

31. Rouanet, A., Contribution a l'étude des systèmes zircone–oxydes des lanthanides au voisinage de la fusion. *Rev. Int. Hautes Temp. Réfract.*, **8** (1971) 161–80.
32. Brown, F. H. Jr. & Duwez, P., The systems zirconia–lanthana and zirconia–neodymia. *J. Am. Ceram. Soc.*, **38** (1955) 95–101.
33. Bastide, B., Odier, P. & Coutures, J. P., Phase equilibrium and martensitic transformation in lanthana-doped zirconia. *J. Am. Ceram. Soc.*, **71** (1988) 449–53.
34. Wilder, D. R., The La_2O_3–ZrO_2 system. In *Phase Diagrams for Ceramists*, Vol. IV, ed. R. S. Roth, T. Negas & L. P. Cook. American Ceramic Society, Columbus, OH, USA, 1981, pp. 133.
35. Korneev, V. R., Glushkova, V. B. & Keler, E. K., Heats of formation of rare earth zirconates. *Izv. Akad. Nauk SSSR, Neorg. Mater.*, **7** (1971) 886–7.
36. Andersson, J. -O., Guillermet, A. F., Gustafson, P., Hillert, M., Jansson, B., Jonsson, B., Sundman, B. & Ågren, J., A new method of describing lattice stabilities. *CALPHAD: Comput. Coupling Phase Diagrams Thermochem.*, **11** (1987) 93–8.
37. Du, Y., Investigation of the ZrO_2–$YO_{1.5}$–CaO–MgO and Co–Ni–Ti phase diagrams. PhD thesis, Central South University of Technology, China, 1992.
38. Gldstein, H. W., Nellson, E. F., Walsh, P. N. & White, D., The heat capacities of yttrium oxide (Y_2O_3), lanthanum oxide (La_2O_3) and neodymium oxide (Nd_2O_3) from 16 to 300 K. *J. Phys. Chem.*, **63** (1959) 1445–9.
39. Justice, B. H. & Westrum, E. F. Jr, Thermophysical properties of the lanthanide oxides. I. Heat capacities, thermodynamic properties, and some energy levels of lanthanum (III) and neodymium (III) oxides from 50 to 350 K. *J. Phys. Chem.*, **67** (1963) 339–45.
40. Basili, R., Sharkawy, A. E. & Atalla, S., Experimental determination of the thermal properties of Nb_2O_5, La_2O_3 and Ce_2O_3 in the temperature range 400–1000 K. *Rev. Int. Hautes Temp. Refract.*, **16** (1979) 331–8.
41. Blomeke, J. O. & Ziegler, W. T., The heat content, specific heat and entropy of La_2O_3, Pr_6O_{11} and Nd_2O_3 between 30 and 900°C. *J. Am. Chem. Soc.*, **73** (1951) 5099–102.
42. King, E. G., Weller, W. W. & Pankratz, L. B., Thermodynamic data for lanthanum sesquioxide. U. S. Bur. Mines, Rept. Invest. No. 5857, 1961, 6. pp.
43. Yashvili, T. S., Tsagareishvili, D. Sh. & Gvelesiani, G. G., Enthalpy and specific heat of the sesquioxides of lanthanum and lutecium at high temperatures. *Teplofiz. Vys. Temp.*, **6** (1968) 817–20.
44. Knacke, O., Kubaschewski, O. & Hesselmarm, K., *Thermochemical Properties of Inorganic Substances*. Springer-Verlag, Berlin, 1991.
45. Shevchenko, A. V. & Lopato, L. M., TA method application to the highest refractory oxide systems investigation. *Thermochimica Acta*, **93** (1985) 537–40.
46. Dinsdale, A., OXUNARY databank, National Physical Laboratory, Teddington, U. K., 1993.
47. Shpil'rain, E. E., Kagan, D. N., Barkhatov, L. S. & Koroleva, V. V., Measurement of the enthalpy of solid and liquid phases of yttria. *High Temp.–High Pressures*, **8** (1976) 183–6.
48. Ferro, R., Delfino, S., Borzone, G., Saccone, A. & Cacciamani, G., Contribution to the evaluation of rare earth alloy systems. *J. Phase Equilibria*, **14** (1993) 273–9.
49. Shannon, R. D., Revised effective ionic radii and systematic studies of interatomic distances in halides and chalcogenides. *Acta Crystallogr., Sect. A*, **32** (1976) 751–67.
50. Wagner, C., *Thermodynamics of Alloys.*, Addison-Wesley Press, Inc., Cambridge, Mass., USA, 1952.
51. Agarwal, R., Fries, S. G., Lukas, H. L., Petzow, G., Sommer, F., Chart, T. G. & Effenberg, G., Assessment of the Mg–Zn system. *Z. Metallkde.*, **83** (1992) 216–23.
52. Du, Y., Yashima, M., Koura, T., Kakihana, M. & Yoshimura, M., Thermodynamic evaluation of the ZrO_2–CeO_2 system. *Scripta Metall. Mater.*, **31** (1994) 327–32.